# Lossless propagation of magnetic dipole excitations on chains of dielectric particles with high refractive index

O. Zhuromskyy and U. Peschel

*Institutes of Optics, Information and Photonics, University of Erlangen-Nuremberg, Erlangen, Germany*

(Received 15 April 2014; revised manuscript received 25 June 2014; published 9 September 2014)

Lossless propagation of longitudinal magnetic dipole waves along chains of high-index subwavelength particles is predicted for a narrow frequency range around the magnetic Mie resonance of the individual particles. Mathematical analogies between dipole and magnetoinductive waves are used to reduce back-reflections thus improving the power transfer efficiency of respective particle waveguides. The proposed technique can be used to optimize the propagation of even more complex particle-based configurations.

DOI: 10.1103/PhysRevB.90.125117 PACS number(s): 42.25.Bs, 73.21.−b

## I. INTRODUCTION

In order to merge electronics and photonics on ever smaller scales, the problem of signal transfer along narrow nanoscaled channels was addressed by various means including dielectric and plasmonic waveguides or nanoantenna based wireless interconnects [1]. Although in terms of propagation loss dielectric waveguides are the clear favorites, technological difficulties connected with the growth and patterning of monocrystalline layers of, e.g., direct semiconductors being capable of providing gain motivate the search for alternative technologies. The concept we explore in the present work relies on dipole excitations propagating along regular chains of subwavelength dielectric particles. Such particles can be produced in a separate technological procedure to be later deposited by self-assembly techniques [2], which gives a possibility to combine high refractive index materials with incompatible chemistry like, for example, silicon and indium phosphate. In addition, the smallest up-to-date lasers are based on the spaser concept and have spherical shape [3], thus can easily be integrated into our concept. Particle chains, as we show, support propagating modes with losses comparable to those of conventional dielectric waveguides. The propagation mechanism is basically the same as in the gold particle chains presented by Quinten *et al*. [4], namely, the dipole excitation is transferred along the chain due to coupling between chain elements. Unfortunately strong material losses of gold and other metals limit the propagation length drastically, a restriction that is lifted for dielectric particles. The lower losses in case of dielectric materials go hand in hand with a reduced field confinement resulting in a larger mode diameter. Another distinction of our concept from that of Quinten is the use of magnetic dipoles instead of electric ones. The quality factor of the electric dipole excitation on dielectric spheres is usually rather low due to radiation losses leading to an enhanced coupling to higher order modes like quadruple, hexapole, and others of the neighbor particles. Thus the intensity of the electric dipole excitation declines rapidly along the chain. In contrast, the overlap of the magnetic dipole mode with higher order multipole modes of neighboring particles is way smaller and thus the dipole excitation can be transmitted almost without attenuation. But, lossless propagation is only one goal to be achieved. Efficient in- and outcoupling are at least equally important for on-chip operation. Here, we show that power insertion into and extraction from coupled chains of spheres can be easily optimized using techniques originally developed for electric transmission lines.

The paper is structured as follows. In Sec. II, the chain waveguide structure and electromagnetic oscillations in it are presented. In Sec. III, dispersion characteristics of the longitudinal magnetic dipole mode are obtained. Power transmission and consumption properties of the chain waveguide are considered in Sec. IV.

## II. PARTICLE WAVEGUIDE

The structure to be investigated is shown in Fig. 1. The waveguide is composed of blue particles and the emitting and absorbing elements are indicated by the yellow and red spheres, respectively. The system can be excited with a nanosized optical light source like, for example, a spaser [5] or a nanolaser [3] with the emitted field coupling to magnetic dipole waves. In Fig. 1, an oscillating electric dipole provides for the magnetic dipole excitation guided along the chain of dielectric particles to an absorbing element, which could be represented by an optical nanoantenna [6], at the opposite end of the chain.

In what follows, we suppose that the spheres are embedded in a homogeneous dielectric matrix as it is usually the case for particles being assembled via a printing technology. For all practical examples, we assume that the chain is composed of silicon spheres in silica environment. No significant changes will occur, if silicon is replaced by other high index materials and in particular by direct semiconductors which potentially can provide gain. The large refractive index step between silicon and silica [7] allows for a good frequency separation between the electric and magnetic dipole resonances. The interaction between light and isolated spherical particles is treated within the Mie theory [8], where the incident, scattered, and internal electric fields are expanded into particle-centered vector spherical harmonics, $\vec{N}_{mn}(k\vec{r})$ and $\vec{M}_{mn}(k\vec{r})$,

$$\vec{E}(\vec{r}) = \sum_{n=1}^{N_T} \sum_{m=-n}^{n} [a_{mn}\vec{N}_{mn}(k\vec{r}) + b_{mn}\vec{M}_{mn}(k\vec{r})], \qquad (1)$$

here $\vec{r}$ is the coordinate vector, $k$ is the wave number of the electromagnetic radiation, and $N_T$ is the truncation number. The vector spherical harmonics $\vec{N}_{mn}(k\vec{r})$ and $\vec{M}_{mn}(k\vec{r})$ are solutions of Maxwell's equations in spherical coordinates. They are often referred to as electric and magnetic multipole

 

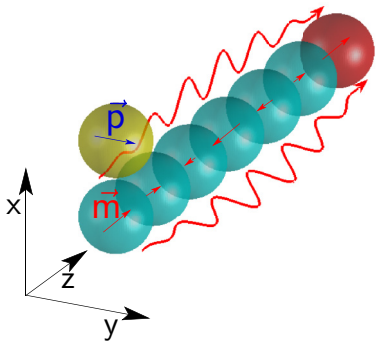


FIG. 1. (Color online) Schematic representation of the particle waveguide.

fields respectively. Following Mie's approach, the expansion coefficients of the scattered fields $a_{nm}$ and $b_{nm}$ can be calculated and scattering cross sections are determined for single spheres. An example calculated for a silicon sphere of 450 nm diameter (for the wavelength dependent refractive indices see Ref. [7]) is displayed in Fig. 2. In the investigated frequency domain, most of the optical response is caused by the resonant excitation of a magnetic dipole mode. The position of the magnetic resonance can be tuned by varying the particle size. However, for smaller particles, the resonance frequencies shift towards shorter wavelengths where the material absorption of silicon is high. Only particles with diameters larger than 250 nm can be well operated in a frequency range where silicon is nonabsorbing. When arranged in a chain the resonances of individual spheres couple and a pass band of magnetic dipole waves appears in the vicinity of the magnetic dipole resonance.

$T$-matrices of a regular array of $N = 250$ silicon particles with a diameter of 450 nm and center to center spacing of 460 nm were computed for a set of wavelengths around the magnetic dipole resonance. To simulate the signal propagation along the particle waveguide, fields were injected by an oscillating electric dipole, where the dipole center is placed one lattice constant away from the first element along the

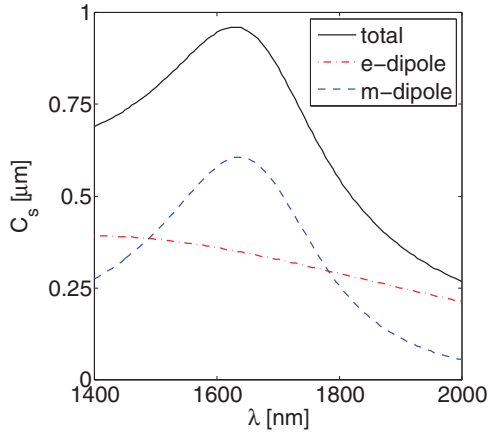


FIG. 2. (Color online) Extinction cross section spectrum of a 450 nm large spherical silicon particle in silica matrix. The solid line is the actual extinction efficiency while the dash-dotted and the dashed lines indicate the electric and magnetic dipole contributions.

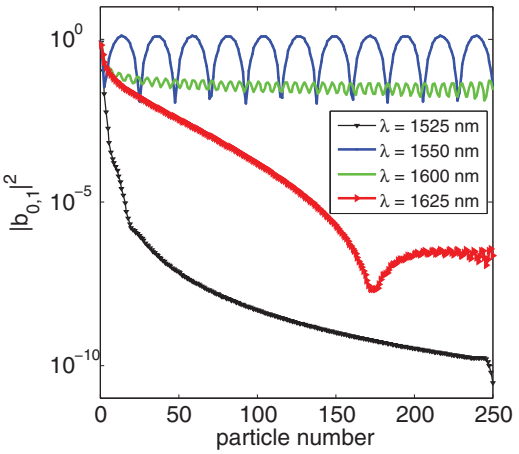


FIG. 3. (Color online) Intensity distribution of the magnetic dipole excitations for a set of wavelengths in a regular chain of 250-silicon particles in silica matrix. The particle diameter $d = 450$ nm and the lattice constant $a = 460$ nm. The chain is excited by an electric dipole placed near the first element as shown in Fig. 1.

$x$ axis and the dipole direction is along the $y$ axis as shown in Fig. 1. In that way, the problem is reduced to a system of linear equations, which is solved by particle related scattered field expansion coefficients as the ones in (1). We discovered that for our specified excitation the only significant excited field amplitudes are those of the magnetic dipoles, $b_{01}^{j}, j = 1,2,\ldots N$, where the index $j$ denotes the position of the sphere within the chain. In comparison, the amplitudes of the other multipoles are at least two orders of magnitude smaller. If we monitor an excitation propagating along a chain of particles (particle diameter $d = 450$ nm, particle center to center spacing $a = 460$ nm) we observe strong dispersive effects (see Fig. 3). Around the resonance of the single-particle, losses are negligible and even beating caused by the strong back-reflection from the end of the chain is clearly visible. In contrast, excitations corresponding to $\lambda = 1500$ and 1625 nm decay rapidly away from the source. This kind of pass-band characteristic is completely unknown for conventional dielectric waveguides, which always support a mode in a symmetric environment.

## III. DISPERSION CHARACTERISTICS

The fact that in the case under consideration only magnetic dipole excitations are present allows us to considerably reduce the system of equations to determine the magnetic dipole amplitudes $b_{01}^{s}(j)$, here the superscript "s" indicates that the amplitude $b_{01}^{s}$ belongs to the induced (or scattered) field expansion whereas the superscript "i" marks amplitudes $b_{01}^{i}$ from the exciting (or incident) field expansion. The equations for $j$th particle in this system has the general form

$$T b_{01}^{s}(j) + \sum_{i=1, i\neq j}^{N} s_{j,i} b_{01}^{s}(i) = b_{01}^{i}(j), \qquad (2)$$

where $T = -1/b_1$ characterizes the particle response to the magnetic dipole excitation with $b_1$ being the Lorenz-Mie

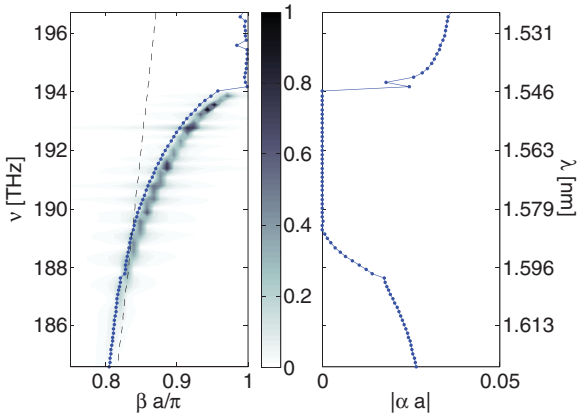


FIG. 4. (Color online) Frequency dependent propagation $\beta$ and attenuation $\alpha$ constants, of a longitudinal magnetic dipole waves propagating along a chain of 450 nm diameter silicon spheres embedded in silica (same parameters as Fig. 3). The contour plot in the left panel shows the normalized Fourier amplitudes of the waves excited in the chain by an electric dipole placed close to one end of the chain. The black dashed curve is the light line, and the lines with filled circles were computed from analytic expressions with 249 interactions accounted for.

coefficient for the magnetic dipole [8]. When excited by a magnetic dipole field centered at the particle, the amplitude of the outgoing magnetic dipole wave is $1/T$. $s_{j,i}$ is the coupling strength between the magnetic dipoles of the $j$th and $i$th particles and mediates the light transport along the chain. Inserting the wave ansatz for the magnetic dipole amplitudes,

$$b^{s}_{01}(j) = \exp(\mathrm{i}kaj), \tag{3}$$

with $k$ being the dipole wave wave number and $a$ the lattice constant, into (2) and setting the external excitation $b^{i}_{0,1}(j)$ to zero results in a dispersion equation for the complex wave number $k = \beta + \mathrm{i}\alpha$. This dispersion equation can be solved numerically for a finite range of significant interactions. In that case, the number of solutions is equal to the number of interactions accounted for. The numerical solution of the obtained dispersion equation with the smallest attenuation constant is plotted for a set of wavelength around the magnetic dipole resonance in Fig. 4. It can be seen that lossless solutions are realized only in the frequency region where the propagation constant $\beta$ leaves the light cone. In this situation, the radiation emitted by the particles interferes destructively in the far field and therefore the electromagnetic energy remains localized in the vicinity of the chain [9]. This result agrees well with the outcome of a Fourier analysis of the field distribution, which is excited into the particle chain by the electric dipole (shadowed background in Fig. 4). Thus the optical response of the chain is well represented by a set of coupled magnetic dipoles.

It should be noted that metallic structures as discussed by Quinten [4] and Engheta [10] operate in a quasistatic regime with mode diameters $d_m$ being a small fraction of the wavelength, $d_m/\lambda \approx 0.15$. Analysis of the computed field distributions in the vicinity of the chain waveguide investigated in this paper give a mode diameter $d_m$ of about 800 nm for $\lambda = 1550$ nm, resulting in $d_m/\lambda = 0.65$. The benefit of this increased mode diameter, which is comparable to the smallest values obtained for conventional silicon waveguides [11], are vanishing propagation losses.

## IV. POWER TRANSFER

In integrated optics the optimization of input and output ports of waveguides is at least as important as the reduction of transmission losses. For example, back-reflection leads to an overall reduction of the energy transfer. In radio-frequency devices, reflections are minimized with the help of matched loads, in optical components antireflection coatings are used. By analogy, in discrete waveguides, reflections can be reduced if not totally eliminated by placing special "matched" particles at the end of the line. The problem of finding the properties of the matched particles is closely related to the boundary layer problem described in the classical book by Brillouin [12]. Elements close to the boundary reflect, because they miss coupling and are therefore in a different situation compared to the elements in the bulk of the lattice. The thickness of the border layer equals the number of elements $N_c$ to which a single sphere is significantly coupled. In order to find the properties of matching particles, which is mainly represented by their magnetic dipole response $T$, a system of equation is formed by writing down Eq. (2) for the last $N_c$ elements of the chain with the excitation terms set to zero. By enforcing the wavelike solution (3), a linear system of equations with $N_c$ unknown matched coefficients $T_j$ is obtained and can be solved. In order to provide for a matched load of the chain, particle shapes and/or material compositions should be tailored such that excited by a magnetic dipole field centered at the particle the amplitude of the scattered magnetic dipole is $1/T_j$. Amplitudes of the other multipoles in the scattered field expansion are not so important because their coupling to the magnetic dipole excitations of neighbors is vanishingly small. For simplicity, let us consider the terminating particles to be spheres with $d = 450$ nm and find permittivities, $\varepsilon_j$, providing the required response, $T_j$. Values of $T = -1/b_1$ for a homogeneous sphere of radius $r$ are given by the analytic expression [13]

$$T = -\frac{\psi_1(\sqrt{\varepsilon}k_0 r)\xi_1'(k_0 r) - \sqrt{\varepsilon}\xi_1(k_0 r)\psi_1'(\sqrt{\varepsilon}k_0 r)}{\psi_1(\sqrt{\varepsilon}k_0 r)\psi_1'(k_0 r) - \sqrt{\varepsilon}\psi_1(k_0 r)\psi_1'(\sqrt{\varepsilon}k_0 r)}, \tag{4}$$

where $\psi_1$ and $\xi_1$ are the Ricati-Bessel functions of the first order, $k_0 = 2\pi/\lambda$ is the electromagnetic wave free space wave number, $\varepsilon$ is the sphere's dielectric constant, and the prime sign indicates the derivatives with respect to the function argument. Permittivities of the last 21 elements that will provide for the perfect matching of the chain are shown in Fig. 5. It should be noted that suppression of back-reflection in a waveguide formed by a particle chain requires amplifying materials with negative imaginary part of the dielectric constant, same as layered perfect absorbers [14,15]. The dielectric constants of the amplifying particles constituting the perfect matching load are indicated in Fig. 5 by red circles.

Although we have neglected all higher multipole moments in the optimization and have only considered the last 20 elements, the reduction of back-reflection is significant (see solid line in Fig. 6). If compared to the free unmatched case (dotted line), the amplitude modulation dropped from 91%

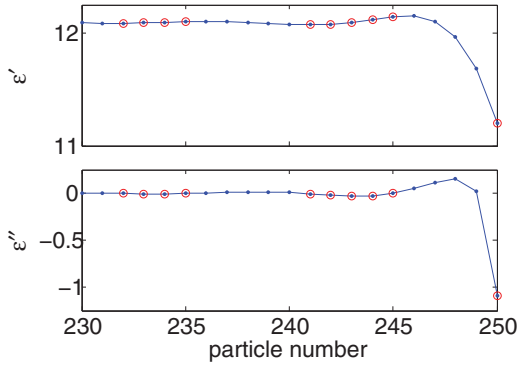


FIG. 5. (Color online) Permittivities of $d = 450$ nm large particles constituting the matched load for the silicon particles chain, real (top) and imaginary (bottom) parts. Circles indicate particles with negative imaginary part of the permittivity.

to below 36%, meaning that the backward reflection reduced from around 70% to less than 5%.

One advantage of waveguiding particle chains is their discrete nature. Additional nanophotonic components as detectors or light sources can be integrated directly into the waveguide provided that their optical properties are adapted respectively. Here we study on the basis of our simplified model how power absorption in a certain particle of the chain can be enhanced by changing its optical properties. Of course, the outcome of this optimization will depend critically on the position of that particular particle inside the chain. For example, their absorption can be enhanced. Contrary to the previous case where properties of a set of particles were changed simultaneously, now the influence of the permittivity change of one single particle in the 250 element chain on the power absorbed by this particular element will be discussed.

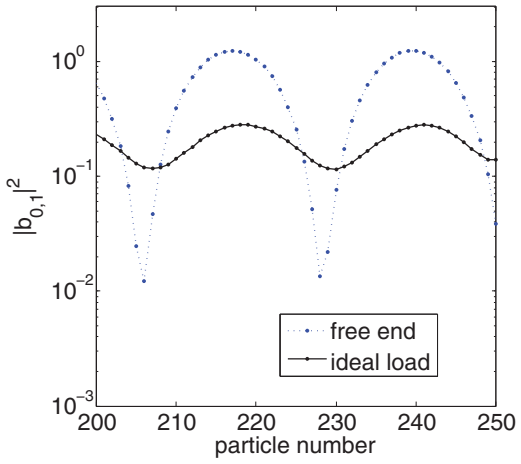


FIG. 6. (Color online) Distribution of the intensity of the magnetic dipole excitation in the closing section of a 450 nm silicon particles chain in silica matrix (dotted line with circles). The solid curve with circles was obtained for the matched load of Fig. 5 with three orders of multipoles in the VSH expansion accounted for. The excitation is provided by an electric dipole close to the chain's first element oscillating at the frequency corresponding to the free space electromagnetic radiation of $\lambda = 1550$ nm.

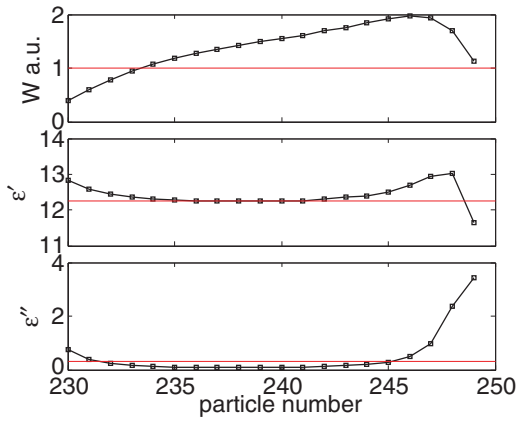


FIG. 7. (Color online) Maximum power absorbed in single-particle absorber vs the its position in the chain of 250 silicon particles. The permittivities of the optimized absorber particles are shown in the middle (real part) and bottom (imaginary parts) panels. The absorbed power is normalized to the absorbed power value in the middle of the chain, and the corresponding permittivity values are marked by the thin horizontal lines. The diameter of the absorber particles equals the diameter of the chain particles $d = 450$ nm, the chain's lattice constant is $a = 460$ nm.

The resulting permittivity values (real and imaginary parts) and the maximum absorbed powers for single point absorbers are shown in Fig. 7 by black squares. The best position for the single particle absorber is in the fifth from the end node, this configuration provides for the highest power throughput along the chain. Here, the permittivity of the 246th element was changed to $\varepsilon_{246} = 12.7 + i0.48$. The presence of an absorbing particle has a dramatic influenced on the field distribution and the power flow. As illustrated in Fig. 8, most of the energy is absorbed in the particle and only about 10% pass it. As compared with the homogeneous chain, the power flow between the emitter and the absorber is almost ten times increased.

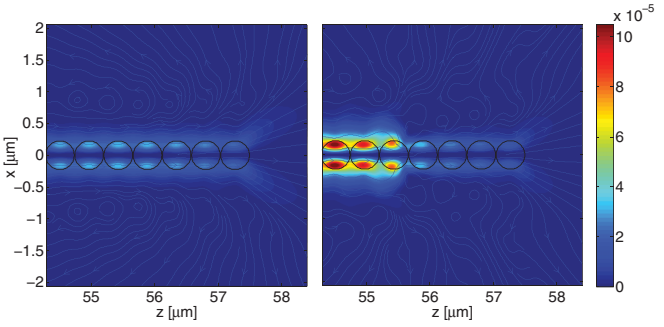


FIG. 8. (Color online) Poynting vector distributions close to the ends of 250 elements long chains of silicon spheres ($d = 450$ nm) excited by an electric dipole at the left-hand side of the chain. The dipole frequency corresponds to the free space wavelength of $\lambda = 1550$ nm. In the structure presented on the right, the element in the 246th position was replaced by the same size spherical particle with $\varepsilon_{246} = 12.7 + i0.48$ providing for light absorption. Streamlines indicate the direction of power flow.

As it can be seen from Fig. 8 there is no radiation along the chain axis, which is another confirmation of the longitudinal polarization of the dipole wave. The main lobe of the radiation pattern is at approximately 30° to the chain axis. Numerical integration of power fluxes shows that in the unloaded case forward radiation amounts to 28% of the incident guided power, where as in the loaded case the number reduces to 12%.

## V. CONCLUSIONS

In our paper, we have shown that discrete particle waveguides allow for lossless propagation of magnetic dipole waves. Starting from $T$-matrix theory we have developed a handy mathematical description to simulate and to optimize the field propagation in such waveguides. We have applied our theory to a chain of silicon nanoparticles embedded in silica and have determined parameters for which back-reflection at the chain ends is minimized or a maximum amount of power is absorbed in a single element of the chain.

## ACKNOWLEDGMENTS

Financial support of the Deutsche Forschungsgemeinschaft (Cluster of Excellence "Engineering of Advanced Materials" and Erlangen Graduate School in Advanced Optical Technologies) is gratefully acknowledged.

[1] A. Alu and N. Engheta, Phys. Rev. Lett. **104**, 213902 (2010).
[2] X. V. Li, R. M. Cole, C. A. Milhano, P. N. Bartlett, B. F. Soares, J. J. Baumberg, and C. H. de Groot, Nanotechnol. **20**, 285309 (2009).
[3] M. A. Noginov, G. Zhu, A. M. Belgrave, R. Bakker, V. M. Shalaev, E. E. Narimanov, S. Stout, E. Herz, T. Suteewong, and U. Wiesner, Nature (London) **460**, 1110 (2009).
[4] M. Quinten, A. Leitner, J. R. Krenn, and F. R. Aussenegg, Opt. Lett. **23**, 1331 (1998).
[5] H. Cao, J. Y. Xu, D. Z. Zhang, S.-H. Chang, S. T. Ho, E. W. Seelig, X. Liu, and R. P. H. Chang, Phys. Rev. Lett. **84**, 5584 (2000).
[6] P. Mühlschlegel, H.-J. Eisler, O. J. F. Martin, B. Hecht, and D. W. Pohl, Science **308**, 1607 (2005); L. Tang, S. E. Kocabas, S. Latif, A. K. Okyay, D.-S. Ly-Gagnon, K. C. Saraswat, and D. A. B. Miller, Nat. Photon. **2**, 226 (2008).
[7] *Handbook of Optical Constants of Solids*, edited by E. D. Palik (Academic Press, San Diego, 1998).
[8] M. Mishchenko, L. Travis, and A. Lacis, *Scattering, Absorption and Emission of Light by Small Particles* (Cambridge University Press, Cambridge, 2002).
[9] C. R. Simovski, A. J. Viitanen, and S. A. Tretyakov, Phys. Rev. E **72**, 066606 (2005).
[10] A. Alù and N. Engheta, Phys. Rev. B **74**, 205436 (2006).
[11] J. T. Robinson, S. F. Preble, and M. Lipson, Opt. Express **14**, 10588 (2006).
[12] L. N. Brillouin, *Wave Propagation in Periodic Structures: Electric Filters and Crystal Lattices* (McGraw Hill, New York, 1946).
[13] C. F. Bohren and D. R. Huffman, *Absorption and Scattering of Light by Small Particles* (Wiley-VCH, Weinheim, 2004).
[14] Y. D. Chong, L. Ge, H. Cao, and A. D. Stone, Phys. Rev. Lett. **105**, 053901 (2010).
[15] W. Wan, Y. Chong, L. Ge, H. Noh, A. D. Stone, and H. Cao, Science **331**, 889 (2011).